

## AMORPHOUS $\text{MoS}_3$ AND $\text{WS}_3$

K. S. Liang, S. P. Cramer, D. C. Johnston, C. H. Chang, A. J. Jacobson,  
J. P. deNeufville and R. R. Chianelli

Corporate Research Laboratories  
Exxon Research and Engineering Company  
Linden, New Jersey 07036, USA

$\text{MoS}_3$  and  $\text{WS}_3$  are examples of a group of transition metal chalcogenides which have only been prepared in amorphous form. Recently these compounds have been found to show interesting properties as cathode materials in ambient temperature alkali metal batteries. In particular,  $\text{MoS}_3$  reacts readily and reversibly with lithium, giving a battery system with a high theoretical energy density. In this paper, we report results of structural studies of amorphous  $\text{MoS}_3$  and  $\text{WS}_3$  using x-ray radial distribution analysis, EXAFS, X-ray photoelectron spectroscopy, magnetic susceptibility measurements and vibrational spectroscopies. The results reveal that these amorphous compounds have a chain-like structure similar to that of the crystalline trichalcogenides of the neighboring IVB and VB elements. However, the combined formations of the metal dimers and polysulfide bonds along the chains are structural features unique to these amorphous compounds. The possible implications of this structure to the observed electrochemical behavior will be discussed.

### INTRODUCTION

The structure of amorphous trichalcogenides of Mo and W of Group VIB have been the subject of several studies<sup>1-5</sup>. The earliest results of these studies suggested that amorphous (a-)  $\text{MoS}_3$  was not an independent compound but a mixture of  $\text{MoS}_2$  and non-crystalline sulfur<sup>1-3</sup>. Later, from analysis of the x-ray radial distribution functions (RDF), Diemann<sup>4</sup> concluded that these amorphous trichalcogenides were genuine compounds, although ambiguities remained concerning their detailed structure. The most recent structural studies on a- $\text{MoS}_3$  and a- $\text{WS}_3$  using high resolution RDF and XPS (x-ray photoelectron spectroscopy) revealed the unique structural features of these compounds. A chain-like structure similar to that of the crystalline trichalcogenides of the neighboring IVB and VB elements was proposed<sup>5</sup>. Along the chain, adjacent metal atoms are bridged with three S atoms. The results also showed dimerization of the metal atoms along the chain and the presence of polysulfide bonds. A formal charge state,  $M^V(\overline{S}_2)_{1/2}$ , for these amorphous trichalcogenides was therefore proposed.

It is interesting to note that the trichalcogenides of Mo and W can only be prepared in amorphous form. These amorphous compounds were reported to have special catalytic properties<sup>6</sup>. More recently, amorphous  $\text{MoS}_3$  was found to have interesting electrochemical properties<sup>7</sup>. a- $\text{MoS}_3$  can react readily and reversibly with more than three lithium atoms per  $\text{MoS}_3$  unit at room temperature. Therefore, a- $\text{MoS}_3$  has potential application as an electrode material for secondary lithium batteries in energy storage. In fact, the electrochemical properties of a- $\text{MoS}_3$  are better than those of the crystalline trisulfides. This study is part of our continuing work aimed at understanding the origin of the unusual electrochemical and catalytic properties of these amorphous compounds.

In this paper, the previously proposed structural model<sup>5</sup> of a- $\text{MoS}_3$  and a- $\text{WS}_3$  will be further refined using EXAFS. The results of magnetic susceptibility measurements and IR and Raman vibrational spectroscopies provide further support of the structural model.

The paper is organized in the following order. Procedures of sample preparation are first presented. The structures of a- $\text{MoS}_3$  and a- $\text{WS}_3$  are then discussed in the next two sections in terms of the local atomic arrangements and the charge states. The former contains the results of RDF and EXAFS analyses and the latter reviews the results of XPS, magnetic susceptibility and vibrational spectroscopic measurements. The paper concludes with a discussion of the structural model and its possible implications with regard to the electrochemical properties of a- $\text{MoS}_3$ .

#### SAMPLE PREPARATION

Amorphous  $\text{MoS}_3$  and  $\text{WS}_3$  used in this study were prepared by thermal decomposition of the ammonium tetrathio compounds<sup>8</sup>,  $(\text{NH}_4)_2\text{MoS}_4$  and  $(\text{NH}_4)_2\text{WS}_4$ , respectively. These tetrathio compounds were prepared by passing  $\text{H}_2\text{S}$  through a solution of ammonium paramolybdate or paratungstate in aqueous ammonia at ambient temperature. Crystals of these salts separated during the reaction. The crystals were removed by vacuum filtration, washed and dried. Compositions of representative batches were checked by chemical analysis. Their x-ray diffraction patterns agreed well with the literature data. The samples were also checked with IR transmission spectra to ensure negligible contamination by oxygen impurities.

The thermal decomposition behavior of the ammonium tetrathio salts is illustrated by a typical thermogravimetric curve in Figure 1. The curve shows a plateau region of temperature near  $325^\circ\text{C}$ , which corresponds to a weight loss of 26.24% from  $(\text{NH}_4)_2\text{MoS}_4$ . This value is close to the theoretical weight loss of 26.16% for the formation of  $\text{MoS}_3$ . The compositions of the amorphous compounds typically obtained are very close to  $\text{MX}_3$  stoichiometry.

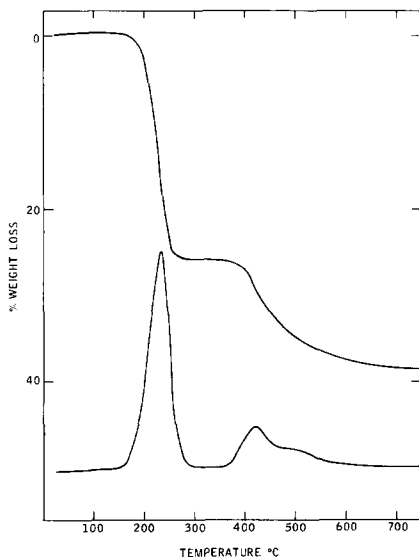


Figure 1

Thermogravimetric decomposition of  $(\text{NH}_4)_2\text{MoS}_4$ , top, thermogram; bottom, differential thermogram

## LOCAL ATOMIC ARRANGEMENTS

The local atomic arrangements of a- $\text{MoS}_3$  and a- $\text{WS}_3$  were studied using x-ray RDF and EXAFS. The experimental details of x-ray RDF have been discussed previously<sup>5</sup>. A detailed description of the EXAFS study will be published separately<sup>9</sup>.

The radial distribution function of a- $\text{WS}_3$  obtained from the x-ray diffraction measurements using  $\text{MoK}\alpha$  radiation is shown in Figure 2. For the following discussion, we are particularly interested in the first three peaks of the RDF which are closely related to the EXAFS results. Using curve fitting with Gaussian peaks the positions, widths and areas of these peaks are obtained (Table 1). As pointed out in our previous paper<sup>5</sup>, the presence of a strong peak at 2.8 Å and only a weak peak at 3.2 Å indicates that a- $\text{WS}_3$  is not a mixture of  $\text{WS}_2$  and S. The proposed structure from our previous work is shown in Figure 3.

We first comment briefly about the interpretation of RDF peaks. Based on a given structure, the theoretical values of the areas of RDF peaks can be calculated from the relation,<sup>10</sup>

$$\rho_{ab}(d) = X_a N_{ab}(d) Z_a Z_b \quad (1)$$

where  $\rho_{ab}(d)$  is the calculated area due to type a atoms coordinated by  $N_{ab}$  type b atoms at a distance d,  $X_a$  is the atomic percent of type a atoms, and  $Z_a$  is the electron density of a type a atom which can be approximated by the atomic number. The calculated values of different atomic pairs are given separately in the Table so that comparisons with the EXAFS results can be easily made later. The S-S pairs are not included because of their small contribution to the RDF areas due to the low Z value of S in comparison with W.

The proposed structure of a- $\text{MoS}_3$  and a- $\text{WS}_3$  is a chain-like structure. This structure in fact is similar to that of the crystalline trichalcogenides of the neighboring groups IVB (Ti, Zr, Hf) and VB (Nb, Ta)<sup>11</sup>. Along the chains, there are alternate short (2.8 Å) and long (3.2 Å) metal-metal distances corresponding to the  $\rho_{W-W}$  values shown on Table 1. Each metal-metal pair is bridged with three S atoms with a metal-sulfur distance of 2.4 Å ( $\rho_{W-S}$  and  $\rho_{S-W}$  on Table 1). The metal-sulfur distance at 2.4 Å and metal-metal distance at 3.2 Å are close to the corresponding interatomic distances in crystalline  $\text{WS}_2$ . However, the short W-W distance of 2.8 Å reveals the formation of metal-metal bonds due to strong metal-metal interaction.

In order to account for the strong RDF peak at 2.8 Å, the proposed structure also includes inter-chain correlations at this distance ( $\rho_{W-S}$  and  $\rho_{S-W}$  at 2.8 Å in Table 1 and Figure 3). Each W would be coordinated with 2 S and one third of the S with 2 W in the adjacent chains to form a super layered structure.

The agreement between the experimental values and the calculated areas of RDF peaks of a- $\text{WS}_3$  based on the above proposed model is reasonably good. The calculated values are larger than the experimental values by ~10% for the 2.4 Å and 3.2 Å peaks. This may partly be due to a density deficiency arising from the porous nature of the thermally decomposed samples. Very intense x-ray scattering at low angles was recently observed on these amorphous samples. Since the small-angle scattering has not been included in our RDF analysis, its effect on the RDF peak area has to be studied<sup>12</sup>. The larger discrepancy shown on the 2.8 Å peak could be due to the disorder of the inter-chain correlation, since the calculation is based on an ordered structure.

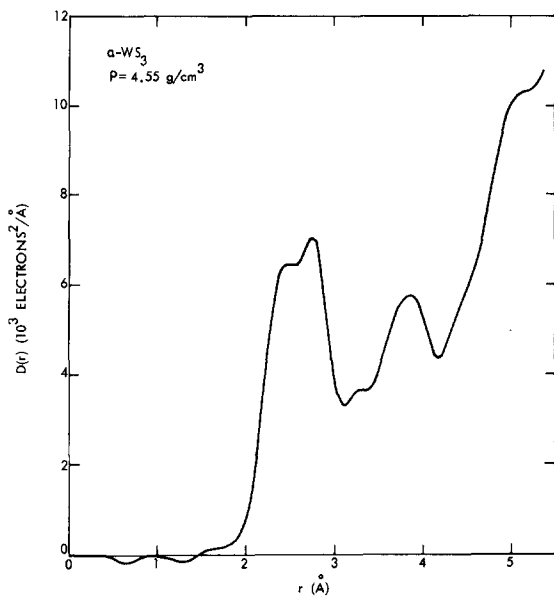


Figure 2

Radial distribution function,  $4\pi r^2 \rho(r)$ , for a- $\text{WS}_3$  obtained from Fourier inversion of the  $\text{MoK}\alpha$  x-ray diffraction data

Table 1  
Coordination Numbers for the Proposed Structure of a- $\text{WS}_3$

Partial RDF	$2.46 \text{ \AA}$	$2.83 \text{ \AA}$	$3.24 \text{ \AA}$
$\rho_{\text{W-W}}$	0	1	1
$\rho_{\text{W-S}}$	6	2	0
$\rho_{\text{S-W}}$	2	2/3	0
Cal. Area	3552	2580	1369
Exp. Area	3261	2029	1237
% Difference	-8.2%	-21.3%	-9.6%

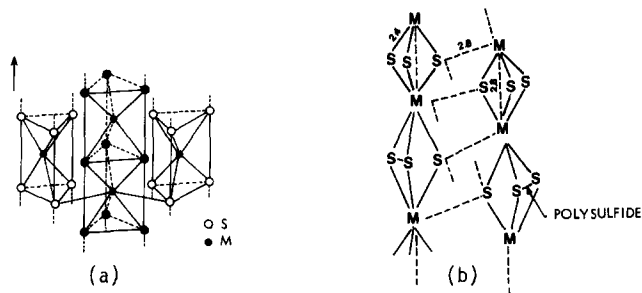


Figure 3

Schematics of (a) the structure of crystalline transition-metal trisulfides and (b) the proposed structure of amorphous  $\text{WS}_3$  and  $\text{MoS}_3$

Due to the fluorescence problem using  $\text{MoK}\alpha$  radiation, the RDF for a- $\text{MoS}_3$  was only obtained using  $\text{CuK}\alpha$  radiation. A broad peak corresponding to the sum of the 2.4 Å and 2.8 Å peaks in the a- $\text{WS}_3$  case was observed at 2.45 Å with a peak area of 2953 electrons<sup>2</sup> (using a density value of 3.04 g/cm<sup>3</sup>). This value is quite close to the calculated value of 3129 electrons<sup>2</sup> based on the above proposed structure.

We now turn our discussion to the EXAFS results. The principle of EXAFS and its application to the study of the local atomic arrangement of amorphous materials have been extensively discussed in the literature<sup>13</sup>. EXAFS can yield accurate interatomic distances ( $\approx 0.02$  Å). If the amplitude functions and the Debye-Waller factors are known, the coordination numbers and mean relative displacements may also be obtained.

For a- $\text{MoS}_3$  and a- $\text{WS}_3$ , EXAFS data using Mo K edge ( $\sim 20,000$  eV) and W L<sub>III</sub> edge ( $\sim 10,205$  eV) were obtained at Stanford Synchrotron Radiation Laboratory. Figure 4 shows the Fourier transform of the Mo K edge EXAFS of a- $\text{MoS}_3$ . The three peaks assigned on the figure were determined through a curve fitting procedure. It should be noted that the positions and origins of these peaks agree with the results of our x-ray RDF analysis.

A simplified version of the curve fitting routine can be described briefly as follows<sup>14</sup>. The fitting is performed with three floating parameters for each shell of the assumed atomic pairs, the coordination number  $N$ , the interatomic distance  $R$ , and the disorder parameter  $\Delta\sigma^2$ , by the following relation

$$\frac{N}{R^2} e^{-\Delta\sigma^2/k^2} A(k)F(k) \quad (2)$$

where  $A(k)$  and  $F(k)$  are the amplitude and phase shift of M-S or M-M pair expressed in functional forms, and  $k$  ( $= [2m(E-E_0)/\hbar^2]^{1/2}$ ) is the photoelectron wave vector. In this study,  $A(k)$  and  $F(k)$  are obtained from the corresponding crystalline disulfides,  $\text{MoS}_2$  and  $\text{WS}_2$ . Since both  $A(k)$  and  $F(k)$  are quite different for M-S and M-M pairs, the peaks in the Fourier transformed EXAFS can be identified quite unambiguously (Figure 4). The results of the fit based on a three-shell model are summarized in Table 2 with the quality of the fit shown in Figures 5 and 6 for a- $\text{MoS}_3$  and a- $\text{WS}_3$ , respectively.

The EXAFS results for a- $\text{MoS}_3$  show that the Mo atoms are coordinated with approximately 5.9 S atoms at 2.41 Å, 0.9 Mo atoms at 2.74 Å and 1.6 Mo atoms at 3.15 Å. This agrees very well with our earlier model. For a- $\text{WS}_3$ , the quality of the curve fit is less satisfactory (Figure 6). This is partly due to the limited k range accessible for curve fitting. The experimental k range is limited by the  $\text{W L}_{II}$  edge at 11542 eV.

An interesting feature of the  $\Delta\sigma^2$  values shown in Table 2 is their negative sign for the M-M shell at 2.74 Å. This sign is consistent with the formation of metal-metal bonds and consequently the reduction of the mean displacements of the metal-metal pairs relative to the crystalline  $\text{MS}_2$  standard.

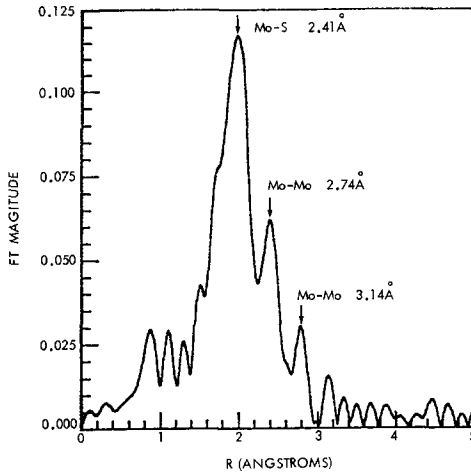


Figure 4

Fourier transform  $\text{MoS}_3$  EXAFS, over  $k = 4-23 \text{ \AA}^{-1}$  with  $k^3$  weighting. All peaks appear shifted from the true distances because of phase shifts.

Table 2  
EXAFS Fitting Parameters

SAMPLE	M-S		M-M(1)		M-M(2)	
	N	$\Delta\sigma^2$	N	$\Delta\sigma^2$	N	$\Delta\sigma^2$
$\text{MoS}_3$	2.414 Å		2.741 Å		3.145 Å	
	5.93	0.0037	0.93	-0.0010	1.63	0.0037
$\text{WS}_3$	2.379 Å		2.757 Å			
	8.11	0.0171	1.30	-0.0030		

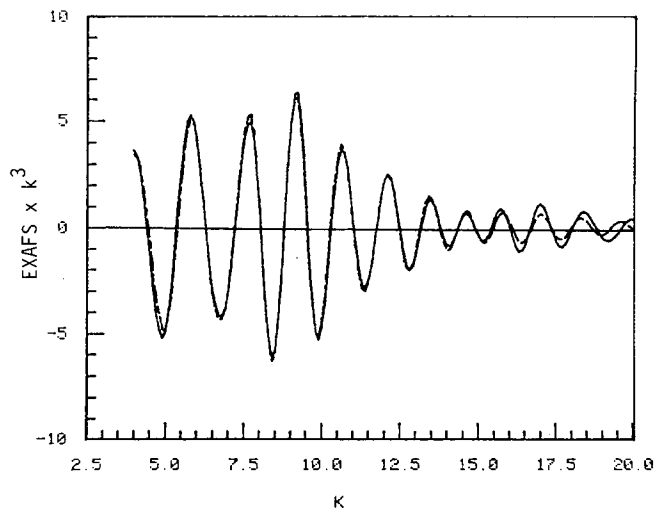


Figure 5  
Fourier-filtered  
EXAFS of  $\text{MoS}_3$  (solid  
line) and fit (dashed  
line)

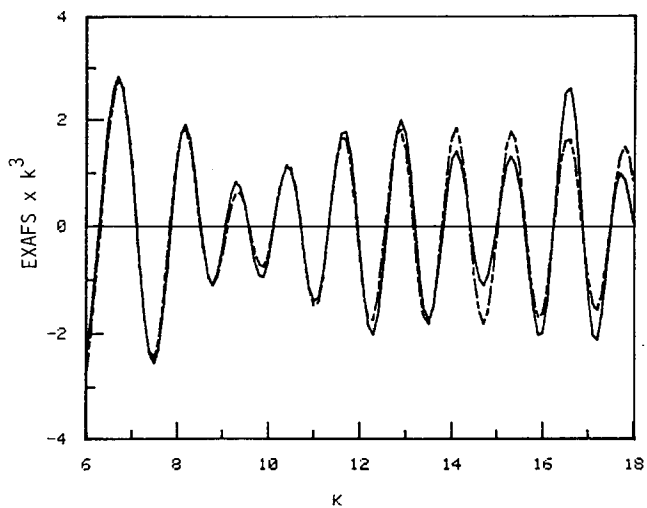


Figure 6  
Fourier-filtered  
EXAFS of  $\text{WS}_3$  (solid  
line) and fit (dashed  
line)

## THE CHARGE STATE

X-ray photoelectron spectroscopy reveals the presence of two types of sulfur species in  $\text{a-MoS}_3$ ,  $(\text{S-S})^=$  and  $\text{S}^=$  with a 1:2 ratio of their intensities (Figure 7). Based on this result, a formal charge state of  $\text{M}^{\text{V}}(\text{S}_2)_{1/2}\text{S}_2^=$  was assigned for these compounds<sup>5</sup>. The spin pairing of  $\text{M}^{\text{V}}$  cations is suggested as the origin of the dimerization of metal atoms in these compounds. Further, the polysulfide species in  $\text{a-MoS}_3$  are present in quite a unique ratio. Presumably, one polysulfide is present in every other bridging sulfur triangle (Figure 3).

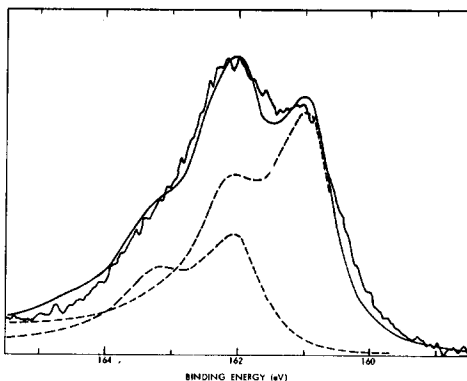


Figure 7

XPS S2p spectrum of amorphous  $\text{MoS}_3$ . Fitted curves correspond to contribution of two types of sulfur, separated by 1.1 eV in binding energy with a 1:2 ratio of intensities

Magnetization measurements were carried out on a variety of high purity samples of  $\text{a-MoS}_3$  in an applied field of 6.35 kG between 10 and 300 K using the Faraday technique. Susceptibilities were extracted from these magnetization data by correcting for the contributions due to ferromagnetic impurities as deduced from magnetization vs. field isotherms obtained at several temperatures for each sample. A brief description of these results is given here; a more complete account and a comparison with previously reported susceptibility data<sup>15,16</sup> on  $\text{MoS}_3$  will appear elsewhere.

Typical susceptibility data are shown in Figure 8. The data were fitted by the following relation,

$$\chi = \chi_0 + \frac{C}{T-\theta}$$

The temperature independent term  $\chi_0$  ( $-61 \times 10^{-6} \text{ cm}^3/\text{mole}$ ), the Curie constant  $C$  ( $7.0 \times 10^{-3} \text{ cm}^3\text{-K}/\text{mole}$ ), and the Weiss temperature  $\theta$  ( $\approx -3 \text{ K}$ ) were determined by a least square fit of the above equation to the data; this fit is shown as a solid line in Figure 8 and in a plot of  $(\chi - \chi_0)^{-1}$  versus temperature in Figure 9. From both figures, the quality of the fit to the data is seen to be excellent.

The value of the Curie constant indicates that this sample contained a level of paramagnetic species which is negligible ( $< 2$  mole %) compared to the Mo content, and therefore is consistent with our structural and formal charge models for  $\text{MoS}_3$  which together require that the  $\text{Mo}^{\text{V}}$  cations be spin paired to form dimers. The magnitude of  $\chi_0$  for  $\text{MoS}_3$  is far smaller than the sum of the molar susceptibilities of crystalline<sup>17</sup> or poorly crystalline<sup>16</sup>  $\text{MoS}_2$  ( $\approx -80 \times 10^{-6} \text{ cm}^3/\text{mole}$ ) and sulfur ( $-15 \times 10^{-6} \text{ cm}^3/\text{mole}$ <sup>18</sup>). This finding provides independent evidence that  $\text{MoS}_3$  is a distinct compound and is not a solid solution of  $\text{MoS}_2$  and sulfur.



Finally, Raman and IR vibrational spectroscopies were also performed to study the local bonding of a- $\text{MoS}_3$ . The results are shown in Figure 10. These spectra bear no common feature to that of crystalline<sup>19</sup> or amorphous<sup>20</sup>  $\text{MoS}_2$ . The presence of a broad band at about  $520\text{ cm}^{-1}$  in both Raman and IR spectra may be due to polysulfide species. Similar S-S stretching frequencies of  $510\text{ cm}^{-1}$  (IR) and  $515\text{ cm}^{-1}$  (Raman) have been observed on a tetramethyl ammonium salt containing polysulfide bonds.<sup>21</sup> These results again confirm that a- $\text{MoS}_3$  is a genuine compound.

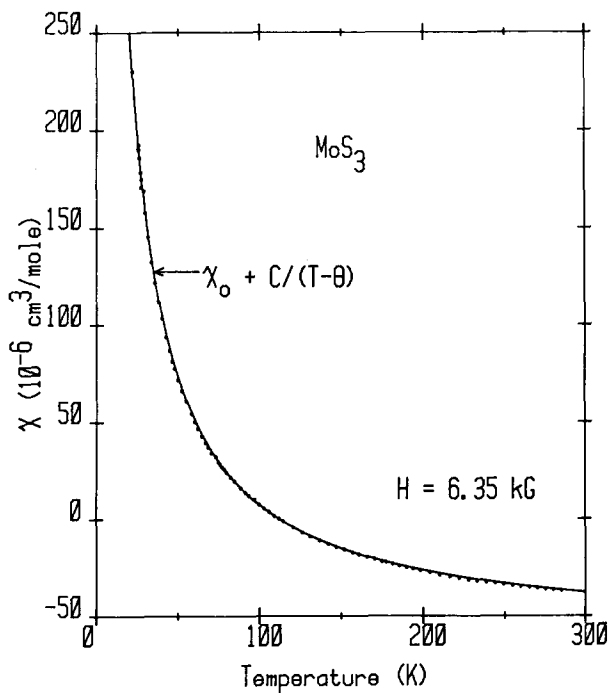


Figure 8

Molar magnetic susceptibility versus temperature for  $\text{MoS}_3$ . The solid curve is a fit of the displayed equation to the data; the fitting parameters  $\chi_0$ ,  $\theta$  and  $C$  are given in the text.

## DISCUSSION

Based on the results of RDF, EXAFS, XPS, magnetic susceptibility measurements and vibrational spectroscopy, we conclude that the amorphous trisulfides of Mo and W are genuine compounds with their own unique structure. We propose a chain-like structure with metal atoms along the chain bridged with three S atoms. The metal atoms in the chain are paired, giving rise to alternate short (2.8 Å) and long (3.2 Å) metal-metal distances. The formation of polysulfide bonds among the S atoms was also observed. These compounds therefore appear to have a unique formal charge state of  $\text{MV}(\text{S}_2)_{1/2}\text{S}_2^-$ . The pairing of MV cations to form dimeric clusters is consistent with the observed magnetic properties of a- $\text{MoS}_3$ .

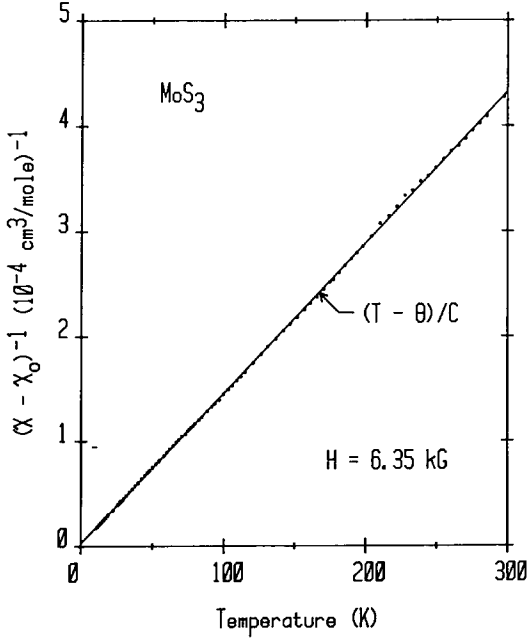


Figure 9

Inverse of the molar magnetic susceptibility of  $\text{MoS}_3$ , corrected for the temperature independent contribution  $\chi_0$ , plotted versus temperature. The solid line is the fit to the data (cf. Fig. 8 caption).

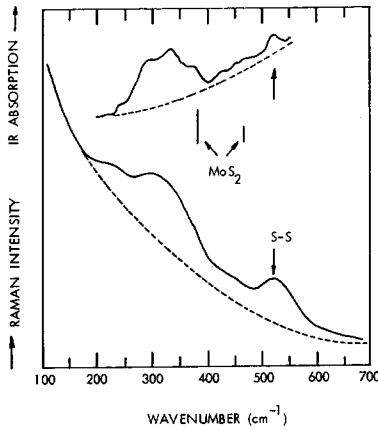


Figure 10

Vibrational spectra of  $\text{MoS}_3$ , top, IR absorption; bottom, Raman intensity. Dotted lines are estimated backgrounds.

As stated in the Introduction, the work presented here is part of a continuing effort aimed at understanding the interesting electrochemical and catalytic properties of these compounds, such as the reversible reaction of Li with a-MoS<sub>3</sub>. We will comment briefly on this reaction.

The chain-like structure of a-MoS<sub>3</sub> is evidently favorable to topochemical reaction with Li. However, by comparing the reversibility of Li reaction in the trichalcogenides and dichalcogenides of both crystalline<sup>22</sup> and amorphous<sup>7,23</sup> forms, the open structure associated with the low-dimensionality of the chains cannot be the primary factor in determining the reversibility of the reaction. In Table 3, some known dichalcogenides and trichalcogenides are grouped roughly into three classes in accordance with the reversibility of their reaction with Li. There appears to be no clear trend associated with the structure. At present, we conjecture that the reversibility might be associated with the electronic nature of these materials. In particular, we feel that the metal-metal bonding and the polysulfide bonds could be important in the reversible reaction with Li. It may be possible to verify this conjecture from structural and other studies on lithiated MoS<sub>3</sub> compounds.

Finally, it should be pointed out that amorphous MoS<sub>2</sub> was also found to react reversibly with Li, although Li does not react topochemically at room temperature with crystalline MoS<sub>2</sub>. In fact, the capacity of Li uptake in MoS<sub>2</sub> was found to decrease continuously with increased crystallinity. Therefore, the role of defect states in the chemistry of Li reaction in these amorphous compounds needs to be addressed.

Table 3  
Reversibility of Li Reaction

<u>Poor</u>	<u>Average</u>	<u>Good</u>
c-MoS <sub>2</sub>	c-NbS <sub>2</sub>	c-TiS <sub>2</sub>
		a-MoS <sub>2</sub>
c-TiS <sub>3</sub>	c-NbS <sub>3</sub>	c-NbS <sub>3</sub>
		a-MoS <sub>3</sub>

#### ACKNOWLEDGMENTS

The authors would like to thank Professors A. Bienenstock, K. Hodgson and S. C. Moss for helpful discussions. Special thanks are due to Dr. F. Betts for assistances with the x-ray diffraction experiments. We are also indebted to SSRL for the EXAFS measurements.

#### REFERENCES

1. R. J. H. Voorhoeve and H. M. B. Wolters, *Z. Anorg. Chem.* **376**, 165 (1970).
2. P. Ratnasamy, L. Rodrique and A. J. Leonard, *J. Phys. Chem.* **77**, 3242 (1973).
3. G. C. Stevens and T. Edmonds, *J. Catal.* **37**, 544 (1975).
4. E. Diemann, *Z. Anorg. Allg. Chem.* **432**, 127 (1977).
5. K. S. Liang, J. P. deNeufville, A. J. Jacobson, R. R. Chianelli and F. Betts, *J. Non-cryst. Sol.* **35** and **36**, 1249 (1980).
6. O. Weisser and S. Landa, "Sulfide Catalysts, Their Properties and Application" Pergamon Press, New York (1973).
7. A. J. Jacobson, R. R. Chianelli, S. M. Rich and M. S. Whittingham, *Mat. Res. Bull.* **14**, 1437 (1979).

8. For a Review, see E. Diemann and A. Muller, *Coord. Chem. Rev.* 10, 79 (1973)
9. S. P. Cramer, K. S. Liang, A. J. Jacobson and R. R. Chianelli, to be published.
10. B. E. Warren, "X-Ray Diffraction", Addison-Wesley Publishing Co., Reading, Massachusetts, 1969.
11. F. Hulliger, "Structural Chemistry of Layered-Type Phases", Ed. F. Levy, D. Reidel Publishing Co., Dordrecht, Holland, 1976.
12. G. S. Cargill III, *J. Appl. Cryst.* 4, 277 (1971).
13. See, for example, S. H. Hunter, A. I. Bienenstock, and T. M. Hayes, in "Structure of Non-Crystalline Materials", edited by P. H. Gaskell, Taylor and Francis, London, 1977.
14. S. P. Cramer, K. O. Hodgson, E. I. Stiefel and W. E. Newton, *J. Am. Chem. Soc.* 100, 2748 (1978).
15. S. Meyer, *Ann. Physik* 69, 236 (1899).
16. P. Belougne and J. V. Zenchetta, *Revue de Chimie Minerale* 16, 565 (1979).
17. R. M. M. Fonville, W. Geertsma and C. Haas, *Phys. Stat. Sol.* (b) 85, 621 (1978).
18. *CRC Handbook of Chemistry and Physics*, 60th Edition, R. C. Weast, Editor, (CRC Press, Boca Raton, Florida, 1979), p. E-127.
19. T. J. Wieting and J. L. Verble, *Phys. Rev.* B3, 4286 (1971).
20. J. S. Lannin, in *Proc. 7th Int. Conf. Amorphous and Liquid Semiconductors*, Ed. W. E. Spear, University of Edinburgh, 1977.
21. W. Rittner, A. Müller, A. Neumann, W. Bäther and R. C. Sharmo, *Angew. Chem. Int. Ed. Engl.* 18, 530 (1979).
22. R. R. Chianelli and M. B. Dines, *Inorg. Chem.* 14, 2417 (1975).
23. A. J. Jacobson, R. R. Chianelli and M. S. Whittingham, *J. Electrochem. Soc.* 126, 2277 (1979).